PHYSICAL REVIEW B VOLUME 61, NUMBER 19 15 MAY 2000-I

Ion-dose-dependent microstructure in amorphous Ge

M. C. Ridgway and C. J. Glover
Department of Electronic Materials Engineering, Australian National University, Canberra ACT 0200, Australia

K. M. Yu
Materials Sciences Division, Lawrence Berkeley National Laboratory, Berkeley, California 94701

G. J. Foran
Australian Nuclear Science and Technology Organization, Menai, Australia

C. Clerc
Centre de Spectrometrie Nucléaire et de Spectrometrie de Masse, Centre National de la Recherche Scientifique, 91405 Orsay, France

J. L. Hansen and A. Nylandsted Larsen
Institute of Physics and Astronomy, Aarhus University, Aarhus, Denmark
(Received 14 February 2000)

Implantation-induced, microstructural modifications including increased bond length and non-Gaussian static disorder have been measured in amorphous Ge using extended x-ray absorption fine-structure spectroscopy. The evolution of the *amorphous phase* interatomic distance distribution as functions of ion dose and implant temperature demonstrates the influence of implantation conditions on *amorphous phase* structure. Results are attributed to increased fractions of three- and fivefold coordinated atoms as a means of accommodating implantation-induced point defects.

Implantation-induced structural changes in semiconductor substrates can include the crystalline-to-amorphous[1] and continuous-to-porous[2] transformations at low ($\sim 10^{14}/\mathrm{cm}^2$) and high ($\gtrsim 10^{16}/\mathrm{cm}^2$) ion doses, respectively. Though such phenomena have been previously investigated, the atomic-scale structure of the *amorphous phase* formed by ion implantation has not been determined in detail nor has the potential influence of the implant conditions on such structure been considered. Herein, we demonstrate that the microstructure of the semiconductor Ge evolves, in the *amorphous phase*, as functions of both ion dose and implant temperature. The four moments of the amorphous-Ge interatomic distance distribution have been determined using extended x-ray absorption fine-structure spectroscopy (EXAFS) and unambiguously show the presence of implant-condition-dependent non-Gaussian static disorder.

EXAFS is a proven technique for the measurement of the structural parameters of disordered materials such as amorphous semiconductors.[3] Of the latter, amorphous Ge has been studied extensively, though conflicting experimental results have been reported due to differences in both data analysis and sample fabrication methodologies.[4] For example, though *crystalline* Ge can be correctly analyzed with the standard EXAFS formalism that assumes a Gaussian distribution of interatomic distances, anharmonicity in the form of non-Gaussian static disorder in *amorphous* Ge can require a model-independent approach to avoid significant errors in analysis.[5] Similarly, with a common analytical methodology,[4] different results have been reported for samples fabricated by sputtering and evaporation. For the present report, the structural parameters of amorphous Ge formed by ion implantation were determined using the model-independent cumulant method.[6] This means of analysis is based on the expansion of the EXAFS amplitudes and phases as a moment series of the interatomic distance distribution and is appropriate for the amorphous-Ge materials system with low to moderate anharmonic disorder.[4]

As demonstrated previously, ion implantation is an effective methodology for the fabrication of amorphous semiconductor EXAFS samples.[7] For the present report, a crystalline Ge layer of thickness $\sim 2\ \mu\mathrm{m}$ was deposited by molecular beam epitaxy at 600 °C on a Si-on-insulator heterostructure [Si(0.2 μm)/SiO_2(0.4 μm)/Si(substrate)]. Samples were annealed both *in situ* and *ex situ* to fully relax the epitaxial layer. The lattice-mismatched Ge layer was then masked with Apezion black wax and detached, with the Si layer of thickness 0.2 μm, from the Si substrate by selective chemical etching of the SiO_2 layer in HF:H_2O (1:2) solution. Utilizing the black wax for structural stability and C dag for electrical and thermal conductivity, the thin Ge layer was then amorphized with a multiple-energy, multiple-dose Ge-ion-implantation sequence. (For the given ion energy and dose combinations,[8] the nuclear energy deposition density was approximately constant over the extent of the Ge layer.) Samples were implanted at both -196 and 21 °C (± 3 °C) with an ion-dose range extending approximately two orders of magnitude beyond that required for amorphization ($\sim 10^{14}/\mathrm{cm}^2$). The amorphous-Ge films were then ground to a fine powder,[9] evenly dispersed in a BN binder, and pressed into an Al support between Kapton films such that $\mu x \sim 1$, where μ is the x-ray attenuation coefficient and x is the effective Ge sample thickness. (A crystalline reference sample

 ©2000 The American Physical Society

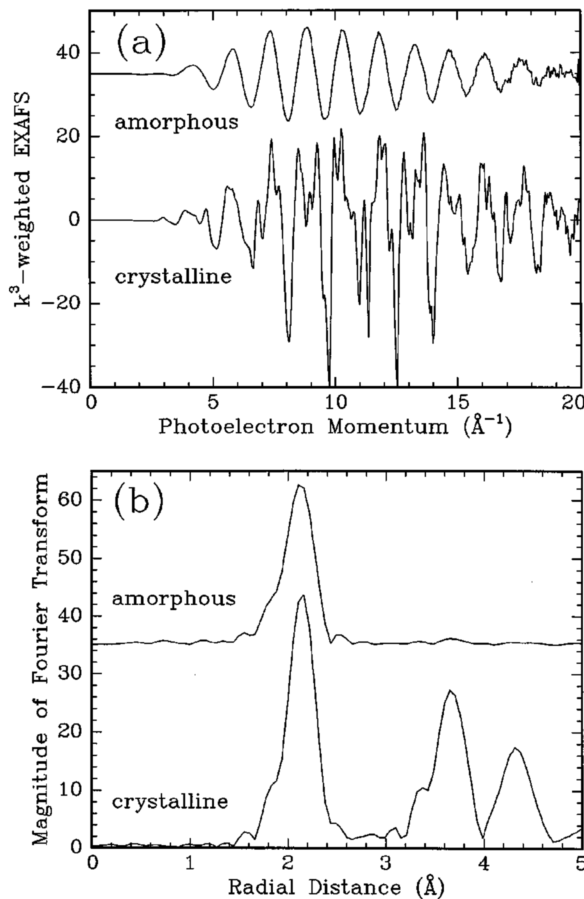

FIG. 1. (a) EXAFS and (b) Fourier-transformed spectra comparing crystalline and amorphized Ge.

was fabricated in an identical manner excluding ion implantation.)

Transmission EXAFS measurements at the Ge K edge were performed on unoxidized samples at a temperature of 12 K at the Stanford Synchrotron Radiation Laboratory (beamlines 2-3 and 4-3) and the Photon Factory, Japan (beamline 20-B). EXAFS data were extracted from the absorption spectra in a conventional manner and for spectral comparison, a common energy origin (E_0) and reference (the absorption-spectra first-derivative maximum) were utilized to align the absorption edges within 0.1 eV. The k^3-weighted EXAFS (where k is the photoelectron momentum) was then Fourier transformed over a k range of 2–16 Å^{-1}.

Figures 1(a) and 1(b) show EXAFS and Fourier-transformed spectra, respectively, for both crystalline and amorphous samples. For the crystalline sample of Fig. 1(a), the complicated EXAFS spectrum resulted from the superposition of the scattering contributions from multiple atomic shells. In the corresponding Fourier-transformed spectrum of Fig. 1(b), first, second, and third nearest neighbors were readily apparent. In contrast, the single-frequency EXAFS spectrum of the amorphous sample was characteristic of scattering from a single shell, and thus only contributions from the nearest neighbors were resolvable in the Fourier-transformed spectrum. Beyond the first shell, disorder-induced broadening of the interatomic distance distribution was sufficient to damp out scattering contributions from next-nearest neighbors. [Note that the EXAFS amplitude for a given shell is proportional to $\exp(-2\sigma^2k^2)$ and the damping due to disorder results from the disorder-induced increase of the Debye-Waller factor (σ^2) value.]

Back-transformed spectra were then calculated using an r-space window over the range 1.73–2.63 Å to extract the separate first-shell amplitude and phase functions required for the cumulant expansion. Following Dalba *et al.*,[4] the coordination number of the amorphized sample (N_s) and the first four relative cumulants (ΔC_i, where $\Delta C_i = C_{i_s} - C_{i_r}$) of the *effective* interatomic distance distribution were calculated from a comparison of the amplitude and phase of an amorphized sample (s) to that of the crystalline reference (r) over the k range 4–14 Å^{-1}. (Specifically, N_s, ΔC_2, and ΔC_4 are determined from the logarithm of the amplitude ratio whilst ΔC_1 and ΔC_3 are determined from the phase difference.[4]) The coordination number (N_r) and bond length (C_{1_r}) of the crystalline reference were set equal to four atoms and the x-ray diffraction standard of 2.4496 Å, respectively. Absolute values of the amorphous-sample cumulants were obtained by adding ΔC_i to the absolute values of the crystalline-reference cumulants, the latter determined assuming a Gaussian interatomic distance distribution. A value of 0.0018 ± 0.0003 Å^2 was determined for C_{2_r} using the XFIT code[10] and errors were calculated by varying E_0 and the windowing conditions over an experimentally meaningful range.

The *real* $[p(r)]$ and *effective* $[P(r,\lambda)]$ interatomic distance distributions with cumulants $C^*_{i_s}$ and C_{i_s} respectively, are such that

$$P(r,\lambda) = p(r)[\exp(-2r/\lambda)]/r^2, \tag{1}$$

with $C_{i_s} \sim C^*_{i_s}$ for $i \geq 2$.[11] The average position of the real distribution $C^*_{1_s}$ was calculated following Ref. 12 wherein a k-independent photoelectron mean free path (λ) of 8 Å was assumed.

Figures 2(a) and 2(b) show examples of the ion-dose and implant-temperature dependence of the structural parameters of amorphized Ge. For an implant temperature of -196 °C, the bond length $C^*_{1_s}$ progressively increased as a function of ion dose with a significantly lesser change apparent for samples implanted at 21 °C [Fig. 2(a)]. In contrast, the Debye-Waller factor $C^*_{2_s}$ (not shown) exhibited no ion-dose or implant-temperature dependence within experimental error. For all amorphized samples, the experimental $C^*_{1_s}$ and $C^*_{2_s}$ values ($\geq 2.458 \pm 0.002$ Å and $\geq 0.0028 \pm 0.0005$ Å^2, respectively) exceeded those of the crystalline reference (2.4496 Å and 0.0018 ± 0.0003 Å^2, respectively). In general, increased values of both bond length and Debye-Waller factor, the latter consistent with the presence of structural disorder, have been reported for amorphous Ge independent of the preparation technique.[4]

The presence of anharmonicity was manifested by nonzero values of the cumulants $C^*_{3_s}$ and $C^*_{4_s}$ which measured, respectively, asymmetric and symmetric deviations of the interatomic distance distribution from Gaussian behavior. From Fig. 2(b), a progressive increase of $C^*_{3_s}$ value as a

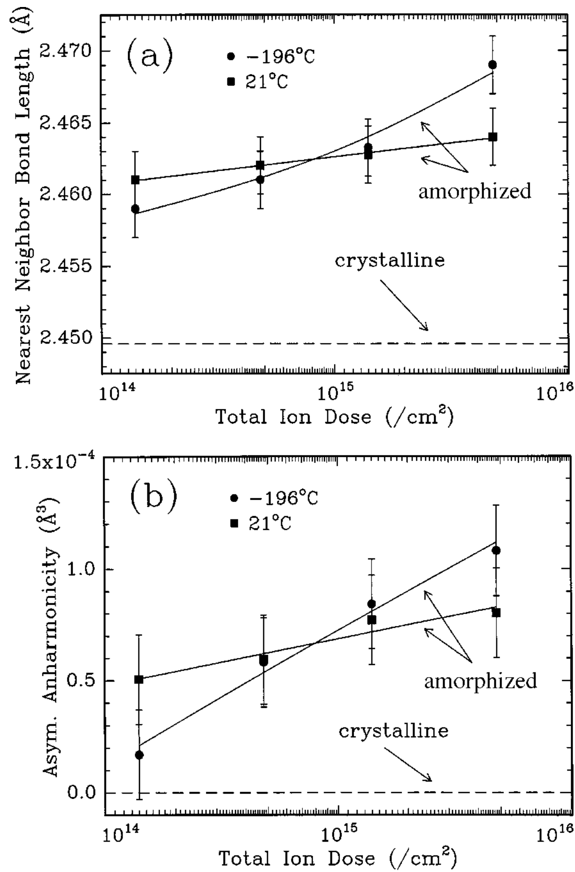

FIG. 2. (a) Nearest-neighbor bond length $C^*_{1_s}$ and (b) asymmetric anharmonicity $C^*_{3_s}$ as functions of ion dose and implant temperature.

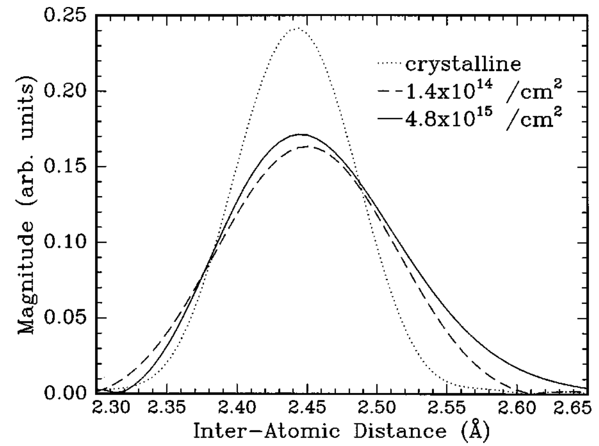

FIG. 3. Real interatomic distance distribution for a pair of nearest-neighbor atoms as a function of ion dose for an implant temperature of −196 °C.

function of ion dose was observed for an implant temperature of −196 °C. As above, a lesser change was apparent for samples implanted at 21 °C. $C^*_{4_s}$ values (not shown) exhibited comparable behavior. For the crystalline reference (where a Gaussian interatomic distance distribution was assumed), $C^*_{3_r}=C^*_{4_r}=0$. In previously published reports, the presence and extent of anharmonicity in amorphous Ge was specific to the fabrication methodology.[4]

In contrast to the results presented above, the first-shell coordination number N_s was, within experimental error, ion-dose *independent* with measured values of 3.82 ± 0.2 and 3.94 ± 0.2 atoms for implant temperatures of −196 and 21 °C, respectively. Such values did not differ from those of the crystalline reference (four atoms) and, though representative of the superposition of all interatomic configurations, were consistent with the general retention of tetrahedral coordination in the local atomic environment as previously reported for amorphous Ge prepared with different techniques.[4]

Figure 3 shows the real distribution of interatomic distances for a pair of nearest-neighbor atoms in amorphous Ge as a function of ion dose. (The implant temperature was −196 °C and for clarity, only the spectra for the two dose extrema have been included.) For the lowest-dose-sample spectrum only, the deviation from a Gaussian distribution was insignificant and as a consequence, analysis with either the standard formalism or cumulant method yielded equal structural parameter values. In contrast, note the asymmetry in the high-dose-sample spectrum or equivalently, the increased proportion of bond lengths greater than the most probable value.

We suggest the observed trends in structural evolution presented in Figs. 2 and 3 were consistent with an implantation-induced increase in the fraction of defective atomic configurations. *Ab initio* molecular-dynamics calculations[12] predict that amorphous Ge is comprised of three-, four-, and fivefold coordinated atoms. Similar concentrations of the two defective configurations (5% and 11% for three- and fivefold coordinated atoms, respectively) result in an average theoretical coordination number of 4.05 atoms, where the three- and five-fold coordinated atom bond lengths (2.52 and 2.57 Å, respectively) exceed the value for the tetragonal site (2.47 Å). An ion-dose-*dependent* increase in the fractions of the two defective configurations should thus yield an increase in average bond length and anharmonicity parameter values (including an increased proportion of bond lengths exceeding the most probable value) yet produce an ion-dose-*independent* coordination number as measured herein.[13] Also, the lesser change in all structural parameter values measured for samples implanted at 21 °C was consistent with increased defect mobility and dynamic annealing relative to a temperature of −196 °C.

Implantation-induced porosity in Ge substrates has been attributed to the nucleation and growth of voidlike cavities via vacancy clustering.[2] Though readily induced at room temperature with ion doses of $\gtrsim 10^{16}/\mathrm{cm}^2$, the onset of porosity has not been observed at −196 °C.[14] At this lower temperature, we suggest the implantation-induced Frenkel-pair components—vacancy- and interstitial-like defects *in the amorphous phase*—that do not recombine may preferentially be accommodated via three- and fivefold coordinated atoms, respectively. The production and retention of such defects in the bulk yields the ion-dose-dependent changes in structural parameter values determined herein using EXAFS. [Note that structural changes were evident using EXAFS at ion doses ($\gtrsim 10^{14}/\mathrm{cm}^2$) significantly less than that required to observe porosity using transmission electron microscopy ($\gtrsim 10^{16}/\mathrm{cm}^2$).[2]] In contrast, implantation-enhanced defect mobility at 21 °C is evidently sufficient to initiate porosity.[14]

At this higher temperature, we further suggest that the vacancy- and interstitial-like defects that do not recombine may, respectively, preferentially diffuse to voidlike sinks and self-anneal through bond rearrangements with nearest neighbors.[15] A reduced fraction of defects was thus retained within the bulk, and, accordingly the change in all structural parameter values was less relative to samples implanted at −196 °C.

Additional evidence for an ion-dose-dependent fraction of defective configurations in amorphous Ge was obtained from Raman measurements.[16] For samples implanted at −196 °C, changes in the frequency and width of the TO-like band were consistent with increased disordering of the amorphous structure as a function of ion dose. Thermal annealing of such defective configurations was also investigated—selected samples used in the present report were subsequently annealed at a temperature (200 °C) which was insufficient to induce recrystallization. Using EXAFS,[17] structural relaxation of amorphous Ge was readily apparent through a reduction in bond length and asymmetry to a common ion-dose-independent, minimum-energy configuration.[18] These observations were consistent with a reduction in the fraction of defective configurations.

In conclusion, EXAFS has been used to characterize implantation-induced, microstructural modifications in *amorphous* Ge. Increases in bond length and anharmonicity were observed without a change in coordination number. The interatomic distance distribution of *amorphous* Ge was shown to evolve as functions of both ion dose and implant temperature, demonstrating the influence of implantation conditions on *amorphous phase* structure. For an implant temperature of −196 °C, we suggest the structural modifications resulted from an implantation-induced increase in the three- and five-fold coordinated atom fractions and represented a mechanism of accommodating vacancy- and interstitial-like defects within the amorphous phase. For an implant temperature of 21 °C, the structural evolution was less as attributed to a reduced fraction of point defects retained within the bulk.

M.C.R., C.J.G, and G.J.F. were supported by the Australian Synchrotron Research Program, funded by the Commonwealth of Australia via the Major National Research Facilities Program. K.M.Y. was supported by the Department of Energy, Office of Basic Energy Sciences. A.N.L. and J.L.H. are supported by the Danish Natural Scientific Research Council. Work was done (partially) at SSRL which is operated by the Department of Energy, Office of Basic Energy Sciences.

[1] T. E. Haynes and O. W. Holland, Appl. Phys. Lett. **59**, 452 (1991), and references therein.

[2] L. M. Wang and R. C. Birtcher, Philos. Mag. A **64**, 1209 (1991), and references therein.

[3] E. D. Crozier, J. J. Rehr, and R. Ingalls, in *X-Ray Absorption: Principles, Applications and Techniques of EXAFS, SEXAFS and XANES*, edited by D. C. Koningsberger and R. Prins (Wiley, New York, 1989), p. 373.

[4] G. Dalba *et al.*, J. Phys.: Condens. Matter **9**, 5875 (1997) and references therein.

[5] P. Eisenberger and G. S. Brown, Solid State Commun. **29**, 481 (1979).

[6] G. Bunker, Nucl. Instrum. Methods **207**, 437 (1983).

[7] M. C. Ridgway *et al.*, in *Application of Synchrotron Radiation Techniques to Materials Science*, edited by S. Mimi *et al.* (Materials Research Society, Pittsburgh, 1998), p. 309.

[8] 0.9, 3.0, and 6.1 MeV at 2.3, 3.4, and $8.6\times10^{13}/\mathrm{cm}^2$, respectively, and multiples thereof.

[9] Note that EXAFS measurements with crushed-powder samples still yield structural parameters characteristic of bulk material.

[10] P. J. Ellis and H. Freeman, J. Synchrotron Radiat. **2**, 190 (1995).

[11] G. Dalba *et al.*, Phys. Rev. B **52**, 149 (1995).

[12] G. Kresse and J. Hafner, Phys. Rev. B **49**, 14 251 (1994).

[13] Note that slight differences in the production rates of the defective configurations would not have been resolvable given the uncertainty in the coordination-number determination.

[14] B. R. Appleton *et al.*, Appl. Phys. Lett. **41**, 711 (1982).

[15] T. K. Chaki and J. C. M. Li, Philos. Mag. A **51**, 557 (1985).

[16] I. D. Desnica-Frankovic (private communication).

[17] C. J. Glover *et al.* (unpublished).

[18] Given the observation of the thermally induced structural relaxation of amorphized Ge at 200 °C, the possibility of structural modification in samples implanted at −196 °C and subsequently stored at room temperature must also be considered. Accordingly, the immediate post-implant state of such samples (at −196 °C) was potentially more defective than that subsequently measured using EXAFS.